HHS Public Access

Author manuscript

Nat Chem Biol. Author manuscript; available in PMC 2015 April 01.

Published in final edited form as:

Nat Chem Biol. 2014 October ; 10(10): 845–852. doi:10.1038/nchembio.1623.

A broad HIV-1 inhibitor blocks envelope glycoprotein transitions critical for entry

Alon Herschhorn[1,2], **Christopher Gu**[1], **Nicole Espy**[1,2], **Jonathan Richard**[3], **Andrés Finzi**[3,4], and **Joseph G. Sodroski**[1,2,5,*]

[1]Department of Cancer Immunology and AIDS, Dana-Farber Cancer Institute, Boston, MA 02215

[2]Department of Microbiology and Immunobiology, Harvard Medical School, Boston, MA 02215

[3]Centre de Recherche du CHUM and Department of Microbiology, Infectiology and Immunology Université de Montréal, Montreal, Quebec, Canada

[4]Department of Microbiology and Immunology, McGill University, Montreal, Quebec, Canada

[5]Ragon Institute of Massachusetts General Hospital, Massachusetts Institute of Technology, and Harvard, Cambridge, MA 02139; and Department of Immunology and Infectious Diseases, Harvard School of Public Health, Boston, MA 02115

Abstract

Binding to the primary receptor, CD4, triggers conformational changes in the metastable envelope glycoprotein (Env) trimer ($gp120_3/gp41_3$) of human immunodeficiency virus (HIV-1) that are important for virus entry into host cells. These changes include an "opening" of the trimer, creation of a binding site for the CCR5 coreceptor, and formation/exposure of a gp41 coiled coil. Here we identify a new compound, 18A (**1**), that specifically inhibits the entry of a wide range of HIV-1 isolates. 18A does not interfere with CD4 or CCR5 binding, but inhibits the CD4-induced disruption of quaternary structures at the trimer apex and the formation/exposure of the gp41 HR1 coiled coil. Analysis of HIV-1 variants exhibiting increased or reduced sensitivity to 18A suggests that the inhibitor can distinguish distinct conformational states of gp120 in the unliganded Env trimer. The broad-range activity and observed hypersensitivity of resistant mutants to antibody neutralization support further investigation of 18A.

*Correspondence: Joseph G. Sodroski, M.D., Dana-Farber Cancer Institute, 450 Brookline Avenue – CLSB 1010, Boston, MA 02215, Phone: (617) 632-3371, Fax: (671) 632-4338, joseph_sodroski@dfci.harvard.edu.

Author contribution

A.H. and J.G.S. conceived and designed the experiments; A.H. and C.G. performed the screening, viral and cell-cell fusion inhibition assays, chimera/mutant Env engineering and antibody binding/inhibition experiments; N.E. performed some of the viability assays; J.R. and A.F. performed some of the Env mutagenesis and experiments assessing CD4-induced conformational changes; A.H., A.F. and J.G.S analyzed data and wrote the paper.

Competing financial interests

The authors declare no conflict of interest.

INTRODUCTION

In the absence of antiviral therapy, infection by human immunodeficiency virus type 1 (HIV-1) typically leads to acquired immunodeficiency syndrome (AIDS) and death[1–2]. Entry of HIV-1 into target cells is mediated by the interaction of the viral envelope glycoproteins (Envs) with the CD4 receptor and either the CCR5 or CXCR4 coreceptor[3–5]. HIV-1 Envs on the surface of virions are trimers consisting of three gp120 exterior glycoproteins non-covalently associated with three gp41 transmembrane glycoproteins. Binding of gp120 to the CD4 receptor initiates the entry process, leading to Env structural rearrangements that: i) reposition the gp120 V1/V2 and V3 regions; ii) expose the coreceptor-binding site of gp120; and iii) form and/or expose the heptad repeat 1 (HR1) coiled coil of gp41[3–6]. Subsequent interaction of gp120 with the coreceptor is thought to trigger the insertion of the hydrophobic gp41 fusion peptide into the target cell membrane and the refolding of the gp41 ectodomain into a very stable six-helix bundle[7–9]. This ordered sequence of events channels the energy difference between the metastable unliganded state of Env and the stable six-helix bundle into the fusion of the viral and cell membranes.

The complex HIV-1 entry process is vulnerable to inhibition by small molecules. Some gp120-directed inhibitors have been used as leads for drug development as well as probes to investigate different Env conformations. NBD-556, a small molecule that targets the CD4-binding site of gp120, was used to demonstrate that the CD4-bound conformation is rarely sampled spontaneously on primary HIV-1 isolates[10–11]. Studies of BMS-806, a potent entry inhibitor, highlighted the importance of CD4-induced formation/exposure of the gp41 HR1 coiled coil in virus entry[12–13]. Several derivatives of both compounds with improved breadth and potency have been developed for potential clinical application[14–16].

Identification of additional small molecules that inhibit HIV-1 Env function remains a high priority, as such compounds may help to define conserved structural sites on Env and novel modes of entry inhibition. Such inhibitors can also serve as leads for the development of novel antiretroviral drugs with high potency and breadth. Here we applied a selectivity analysis to focus on the most specific hits from a high-throughput screen, and identified a new compound, 18A (**1**), that inhibits the entry of diverse primary HIV-1 isolates. We defined the preferred Env conformation and mechanism of action of 18A, providing new insights into the ability of small molecules to modulate the activity of HIV-1 Envs.

RESULTS

Selectivity analysis identifies HIV-1 fusion inhibitors

To identify new molecules that potentially affect HIV-1 entry, we established a cell-cell fusion assay that mimics the entry of HIV-1 into cells (Fig. 1a). The assay uses a firefly luciferase (F-luc) readout to measure the fusion of HeLa effector cells that express the Envs from a primary HIV-1 strain and target cells coexpressing the CD4 and CCR5 receptors. As a control assay designed to evaluate the specificity of each compound, HeLa cells were induced to express the F-luc reporter protein. The two assays were validated with known inhibitors, confirming that off-target compounds decreased the readout of both assays, whereas known HIV-1 entry inhibitors selectively inhibited the fusion assay (Fig. 1b and

Supplementary results, Supplementary Fig. 1). Thus, combining the two assays enabled us to distinguish fusion inhibitors from cytotoxic and non-specific compounds.

The cell-cell fusion and control assays were used in parallel to screen 212,285 compounds (Supplementary Tables 1 and 2, Supplementary Fig. 2), and readouts from the two assays were integrated to analyze the activity of each compound. Plotting the effect of each compound on the control readout versus its effect on the fusion readout allowed us to compare the selective inhibition of the compounds (Fig. 1c). Fusion inhibitors that exhibited high specificity localized in the top left portion of the plot; these were identified by using an inhibitory cutoff to sort active compounds and a selectivity threshold to retain the most specific ones (Fig. 1c). Compounds satisfying both criteria were retested (Supplementary Fig. 2) and a group of compounds, which share a common acyl hydrazone core and an adjacent aromatic ring (Fig. 1d and Supplementary Fig. 3), was identified. The most effective compound, 18A, specifically inhibited cell-cell fusion and HIV-1 infection mediated by HIV-1_{JR-FL} and HIV-1_{AD8} Envs (Fig. 2a and b, Supplementary Fig. 3, and see below).

Compound 18A inhibits a wide spectrum of HIV-1 isolates

The effect of 18A on viral infection was tested using recombinant HIV-1 pseudotyped with the envelope glycoproteins of different primate immunodeficiency viruses or the amphotropic murine leukemia virus (A-MLV) as a control. 18A efficiently inhibited infection of CCR5-tropic (R5) HIV-1 strains from phylogenetic clades A, B, C and D (Fig. 2b and Supplementary Table 3). Inhibition of HIV-1 from clade CRF01_AE and of HIV-2_{UC1} was less potent but statistically significant (Supplementary Table 3). HIV-1_{JR-FL}, which was used for the initial screen, was one of the most sensitive strains with a half-maximal inhibitory concentration (IC_{50}) value of 3.6 μM, whereas the dual-tropic HIV-1_{KB9} and the SIV_{mac239} isolates were relatively resistant to inhibition (Supplementary Table 3). Notably, 18A effectively inhibited a wide spectrum of diverse HIV-1 strains, including transmitted/founder[17] and primary isolates, with an average IC_{50} of 6.4 μM for all CCR5-using HIV-1 isolates; the majority (66%) of these CCR5-using isolates demonstrated IC_{50} values less than 6 μM (Supplementary Table 3). The half-maximal cytotoxic concentration (CC_{50}) of 18A for the CD4/CCR5-expressing target cells in the assay was 44 μM, consistent with the observed IC_{50} of 56 μM for the control A-MLV (Fig. 2b and Supplementary Table 3). Importantly, A-MLV infection was not significantly affected by 18A at a concentration of 17 μM, which almost completely blocked HIV-1_{JR-FL} infection (residual infection <10%, Fig. 2b).

The effect of 18A on CXCR4-tropic (X4) viruses was tested using Cf2Th target cells expressing CD4 and CXCR4. The laboratory-adapted HIV-1_{HXBc2} and HIV-1_{MN27} from clade B showed similar inhibition profiles, with IC_{50} values of ~25 μM (Fig. 2c and Supplementary Table 3). Similar concentrations of 18A were required to inhibit the dual-tropic HIV-1_{KB9} isolate in CD4/CXCR4-positive target cells (Supplementary Table 3). The measured CC_{50} of 18A was 63 μM, confirming that the observed 18A inhibition of HIV-1 infection of cells expressing CD4 and CXCR4 is specific and statistically significant. Of note, 18A inhibited infection of Cf2Th-CD4/CXCR4 cells by the chimeric

YU2(HXV3+R440E) virus with an IC_{50} similar to that of the parental R5 YU2 virus infecting Cf2Th-CD4/CCR5 cells; therefore, infection of CXCR4-expressing cells by X4 viruses is not necessarily less sensitive to 18A inhibition than infection of CCR5-expressing cells by R5 viruses. Moreover, as CCR5 and CXCR4 are structurally distinct, 18A inhibition of HIV-1 infection is unlikely to depend on binding these coreceptors.

We next tested the activity of 18A in primary $CD4^+$ T cells (human PBMC), which express lower levels of CD4 and CCR5 on their surface compared to the Cf2Th cells and represent more physiologically-relevant target cells. Inhibition of HIV-1_{JR-FL} infection by 18A was even more potent under these conditions with an IC_{50} of 0.4 μM and complete suppression at 10 μM (residual infection < 5%) (Fig. 2d). No significant effect on A-MLV infection or on the viability of the cells was observed within the range of tested concentrations. In summary, 18A exhibited broad-range and specific inhibition of CCR5- and CXCR4-tropic HIV-1 (Fig. 2b–e).

Target for 18A inhibition

To study the target of 18A inhibition, we constructed chimeric Envs between the Env of HIV-1_{JR-FL}, one of the most susceptible strains, and that of HIV-1_{KB9}, a relatively resistant strain. An Env with the JR-FL gp120 and the KB9 gp41 was nearly as sensitive as the parental JR-FL Env to inhibition by 18A (Fig. 3a). By contrast, an Env containing the KB9 gp120 and the JR-FL gp41 was about 5-fold less susceptible to 18A inhibition than the JR-FL Env, and slightly more sensitive (2-fold) than the parental KB9 Env. Thus, gp120 is the major determinant of sensitivity to 18A. A chimera in which the major variable loops of JR-FL gp120 were grafted onto the KB9 Env was nearly as sensitive to 18A inhibition as JR-FL, indicating that the major variable regions of gp120 significantly contribute to 18A sensitivity (Fig. 3a).

The contribution of CD4 to inhibition was measured by testing the effect of 18A on the infection of a CD4-independent virus. Productive infection of wild-type HIV-1_{ADA} requires expression of both CD4 and CCR5 on target cells, but the HIV-1_{ADA} N197S Env mutant does not require CD4 and infects CCR5-expressing target cells[18]. The entry of both isolates into CD4/CCR5-expressing cells was blocked by 18A with a similar profile of inhibition, indicating a comparable susceptibility of both viruses to 18A (Fig. 3b). Moreover, 18A protected CD4-negative, CCR5-expressing cells from infection by HIV-1_{ADA} N197S, demonstrating that inhibition does not depend on the presence of CD4.

To test possible contacts of 18A with complex glycans on HIV-1 Env, we produced HIV-1 virions in the presence of two glycosidase inhibitors. Neither treatment had a significant effect on 18A inhibition of viruses with the JR-FL Env (Fig. 3c). Apparently, complex glycans are not required for the binding of 18A to the envelope glycoproteins or for HIV-1 inhibition by 18A.

Reversible interaction of compound 18A with gp120

Inhibition of HIV-1 infection by 18A was reversible. Washing out 18A before infection with HIV-1 virions alleviated any blocking effect of the inhibitor (Supplementary Fig. 4a). In addition, similar IC_{50} values were measured for different levels of infection by HIV-1

(Supplementary Fig. 4b). These results are consistent with a reversible mechanism of inhibition.

To study the interaction of 18A with gp120, we measured the binding of a panel of monoclonal antibodies with known epitopes[19–22] to HIV-1 gp120 in the presence or absence of 18A. The binding of most antibodies was not affected by preincubation of gp120 with 18A (Fig. 3d). A modest but reproducible decrease in the binding of the E51, 17b and 412d antibodies was detected. The E51, 412d and 17b antibodies bind discontinuous CD4-induced (CD4i) gp120 epitopes that overlap the CCR5-binding site and include the highly conserved sequence IKQI (residues 420–423)[21] located in the β20 strand of gp120[23]. Evaluating each group of antibodies separately showed that the effect of 18A on the CD4-induced antibodies was unique and statistically significant (Fig. 3e). A direct interaction of 18A and gp120 was further supported by circular dichroism spectroscopy (Fig. 3f).

The effect of 18A on the binding of gp120 to the CCR5 coreceptor in the absence and presence of soluble CD4 was tested (Supplementary Figs. 5 and 6). No effect of 18A on CCR5 binding was observed.

Susceptibility of HIV-1 gp120 mutants to 18A inhibition

To investigate the interaction of 18A with HIV-1 Env, we tested the sensitivity of a large panel of HIV-1_{JR-FL} and HIV-1_{YU2} Env mutants to inhibition by 18A. Consistent with its wide spectrum of inhibition of primary HIV-1 isolates (Supplementary Table 3), 18A inhibited all of the mutants, including several BMS-806-resistant mutants, to some extent (Supplementary Table 4).

Hypersensitivity of several mutants to 18A was observed, with IC_{50} values decreasing to 5-fold lower than that of the corresponding wild-type Env. Changes associated with hypersensitivity mapped to the α1 and α5 helices of the inner domain, the V2 region, and the β20-β21 element of gp120. Up to 5.2-fold decreases in susceptibility to 18A were also observed and were associated with changes in two regions of gp120: the β20-β21 strands and the V1/V2 variable region. Of interest, the β20-β21 and V1/V2 variable regions are proximal on an available model of the Env trimer[24] (Fig. 4a).

To explore the basis of decreased susceptibility, we evaluated the effect of the changes associated with 18A sensitivity on the reactivity of HIV-1 Env. Env reactivity describes the propensity of Env to change conformation from the metastable unliganded state to downstream conformations such as the CD4-bound state. HIV-1 variants with high Env reactivity typically exhibit increased sensitivity to inactivation by soluble CD4 (sCD4), antibodies, and incubation in the cold[25]. We examined the relationship between susceptibility to 18A and sensitivity to soluble CD4 (sCD4), cold and antibodies. Low susceptibility to 18A inhibition correlated with sCD4 reactivity and with cold sensitivity (Fig. 4, b and c). Evaluating the presence of both properties in each mutant suggests that viruses with reduced susceptibility to 18A inhibition generally exhibit high Env reactivity[26], with enhanced sensitivity to sCD4 inhibition and to cold inactivation (Supplementary Fig. 7a). This implies a preference of 18A for the unliganded state of HIV-1 Env.

The higher reactivity of Env mutants with reduced susceptibility to 18A predicts that they will more readily assume the CD4-bound conformation. Thus, these viruses should be more sensitive to neutralization by antibodies directed against the CD4-induced (CD4i) and V3 epitopes, which overlap the coreceptor-binding site of gp120 that is induced by CD4 binding[23,27]. Compared with Env variants displaying high susceptibility to 18A inhibition, the less sensitive mutants were more efficiently neutralized by the CD4i antibody, 17b, and the V3-directed antibody, 19b (Fig. 4d,e). The 2G12 antibody, which is minimally affected by changes in HIV-1 Env reactivity[28], neutralized both groups of viruses equivalently well regardless of their sensitivity to 18A (Supplementary Fig. 7b). Thus, viruses with reduced susceptibility to 18A inhibition were more sensitive to 17b and 19b neutralization, supporting the hypothesis that these mutants exhibit higher Env reactivity and are more prone to sample the CD4-bound conformation (Supplementary Fig. 8).

We found that some HIV-1_{AD8} Env variants that were previously shown to differ in Env reactivity were nonetheless equally sensitive to 18A inhibition (Supplementary Fig. 9). Therefore, increases in Env reactivity do not necessarily decrease HIV-1 susceptibility to 18A inhibition; the HIV-1 mutants identified herein that display a reduced sensitivity to 18A thus represent only a subset of the Env variants with high Env reactivity.

Effect of 18A on conformational transitions of HIV-1 Env

To gain insight into the mechanism of 18A inhibition of HIV-1 entry, we studied the effect of 18A on the conformation of the HIV-1 Env trimer. The functional, unliganded state of Env is relatively resistant to cold inactivation compared with the CD4-bound Env intermediate[29]. HIV-1_{HXBc2}, a relatively cold-sensitive HIV-1 isolate with a high Env reactivity[29–30], displayed decreased sensitivity to cold inactivation in the presence of 18A compared to viruses treated with the controls, DMSO or unrelated compounds (Fig. 4f). These results suggest that 18A can stabilize the unliganded, functional state of Env during a prolonged exposure to cold.

We next examined the ability of 18A to interfere with the transition of HIV-1 Env from the unliganded state to the CD4-bound conformation. Binding to CD4 triggers conformational changes in Env that result in an “open” conformation in which the CCR5-binding site on gp120 and the HR1 coiled coil on gp41 are formed and exposed. The CD4-induced opening of the Env spike involves a rearrangement of the membrane-distal trimer association domain of gp120 at the trimer apex; the trimer association domain is composed of the V1/V2 and V3 variable regions of gp120. CD4-induced rearrangement of the V1/V2 region results in a decrease in the binding of the PG9 antibody, which recognizes a V1/V2 epitope that is strongly influenced by quaternary structure[31–34]. The sCD4-induced reduction in PG9 binding was observed for either full-length or cytoplasmic tail-deleted Env complexes expressed on the surface of 293T or HOS cells; similar results were obtained with Envs derived from wild-type HIV-1_{YU2} or an HIV-1_{JR-FL} variant with E168K + N188A changes in V1/V2, which restores the integrity of the PG9 epitope in that HIV-1 strain[31–32] (Supplementary Fig. 10). In the absence of sCD4, the PG9 antibody bound to Env-expressing cells, as shown for the cells expressing the HIV-1_{JR-FL} E168K + N188A variant in Fig. 5a. Treatment with 18A did not affect this basal level of PG9 binding. Prior

incubation of Env-expressing cells with sCD4 substantially decreased PG9 binding (from 37.6% to 6.6%). Importantly, addition of 18A prior to sCD4 incubation restored most of the binding signal of PG9 (from 6.6% to 24.1%) without decreasing CD4 binding (Fig. 5a). This effect required incubation with 18A prior to the addition of sCD4 and was consistent over a range of 18A and sCD4 concentrations (Supplementary Fig. 10). These results suggest that 18A inhibits to some extent the CD4-induced conformational rearrangement of the gp120 V1/V2 region.

The transition of HIV-1 Env from the unliganded state to the CD4-bound conformation also involves the CD4-induced exposure of the gp41 HR1 region[7]. To examine the effect of 18A on this process, we used a fusion protein (C34-Ig) consisting of an immunoglobulin Fc and the gp41 HR2 peptide, which recognizes the HR1 coiled coil. No C34-Ig binding was detected without prior incubation with sCD4 (Fig. 5b). Approximately 37% of the Env-expressing cells bound C34-Ig after preincubation with sCD4. Incubation of the cells with 18A prior to sCD4 addition significantly decreased C34-Ig binding in a dose-dependent manner, with only 4.7% of the cells binding C34-Ig at a 100 μM concentration of 18A. Washing out the compound after sCD4 binding did not reverse the effect, excluding any direct interference of 18A with C34-Ig binding to HR1 (Supplementary Fig. 10). Taken together, we conclude that 18A does not interfere with Env binding to CD4 and CCR5, but efficiently blocks two CD4-induced conformational changes in Env: 1) rearrangement of the gp120 V1/V2 region; and 2) formation/exposure of the gp41 HR1 region. CD4 induction of other Env elements, such as the 17b epitope, is unaffected by 18A (see below).

We next examined the effect of 18A on Env recognition by anti-gp120 antibodies, with and without prior addition of sCD4. Consistent with the 18A-mediated decrease of the binding of the CD4i antibody 17b to soluble gp120, a reduction in 17b binding to the cell surface-expressed Env trimer was observed in the presence of 18A (Fig. 5c). As expected, incubation with sCD4 resulted in an increase in 17b binding; 18A did not affect this process, suggesting that the partial inhibition of V1/V2 movement by 18A does not interfere with formation or exposure of the 17b epitope. We also examined the binding of a V3-directed antibody 19b and two antibodies, 2G12 and PGT121, directed against carbohydrate-dependent gp120 epitopes. As expected[19,35], sCD4 reduced the binding of the PGT121 antibody to Env. No significant effect of 18A on the binding of 19b and 2G12, or on the sCD4-induced decrease of PGT121 binding, was observed.

We studied the mechanistic basis of 18A resistance by testing the ability of Env mutants displaying reduced sensitivity to 18A to complete the above conformational rearrangements in the absence and presence of 18A (Fig. 5d-f and Supplementary Fig. 11). As was seen for the wild-type HIV-1_{JR-FL} Env, binding of PG9 to Env mutants with reduced sensitivity to 18A was not significantly affected by 18A (Fig. 5d). Preincubation with sCD4 reduced PG9 binding to most of the Env mutants and this effect was significantly enhanced for the I154A, N156A, L193A and M434A mutants relative to the wild-type Env. 18A-mediated restoration of PG9 binding was very low in these mutants, pointing to a possible pathway to reduce Env susceptibility to the compound (Fig. 5d and Supplementary Fig. 11). Interestingly, the basal level of PG9 binding to the Y435A mutant was low and insensitive to sCD4 preincubation and to incubation with 18A. We also examined the CD4-induced formation/exposure of the

gp41 HR1 coiled coil on the Env mutants with lower 18A sensitivity, in both the absence and presence of 18A. The N156A and M434A mutants were relatively resistant to the blocking effect of 18A on gp41 HR1 exposure (Fig. 5e). Quantitative analysis demonstrated that the levels of gp120 V1/V2 rearrangement and gp41 HR1 exposure in the presence of 18A both contribute to lower susceptibility to 18A (Fig. 5f). Thus, mutants with decreased sensitivity to 18A may use different pathways to reduce their vulnerability to 18A and are apparently able to undergo rearrangements of the gp120 V1/V2 and gp41 HR1 regions even in the presence of 18A.

DISCUSSION

We report the identification of a novel compound, 18A, that exhibits broad inhibitory activity against diverse HIV-1 strains by blocking the function of Env. The HIV-1 Env trimer is a membrane-fusing molecular machine with high potential free energy, and 18A inhibits CD4-triggered conformational changes in this machine that are critical for membrane fusion and virus entry (Fig. 6a). One change involves the rearrangement of the gp120 V1/V2 region, which is located in the trimer association domain at the trimer apex. The CD4-induced “opening” of the HIV-1 Env trimer results in gp120 movement/rotation away from the trimer axis[36]. During this process, the V1/V2 region relocates to near domain 1 of the bound CD4 molecule, while the V3 region projects towards the target cell to interact with the coreceptor. 18A specifically interferes with the relocation of the V1/V2 regions, which make important contributions to the PG9 epitope, without any apparent effect on the CD4-induced movement of the V3 region. A second CD4-induced change that is inhibited by 18A, the formation/exposure of the gp41 HR1 coiled coil, is also blocked by BMS-806[13]. Despite this similarity between 18A and BMS-806, several features distinguish these compounds: i) Although 18A is less potent than BMS-806, 18A has much broader inhibitory activity, inhibiting infection even of an HIV-2 isolate; ii) 18A weakly stabilizes the unliganded state of HIV-1 Env, whereas BMS-806 does not; and iii) 18A inhibits two different rearrangements involved in the transition to the CD4-bound conformation. Thus, the discovery of 18A may represent a good starting point for the development of new, dual-effect blockers that exhibit both potency and breadth.

18A inhibits a wide spectrum of HIV-1 strains, suggesting that it interacts with a conserved site on HIV-1 Env. Although more work is needed to define the site of 18A interaction with Env, the genetic mapping of 18A susceptibility determinants to the gp120 β20-β21 strands and variable regions, particularly V1/V2, and the moderate blocking effect of 18A on CD4i antibody binding are suggestive. In all current models of the HIV-1 Env trimer, the gp120 β20-β21 strands, which critically contribute to the epitopes of all CD4i antibodies, are adjacent to the trimer apex, where the V1/V2 regions reside. A binding site in this locality could explain the observed ability of 18A to impede the CD4-induced down-regulation of the PG9 epitope, which involves movement of the V1/V2 region. The critical site of 18A interaction must be well conserved in HIV-1 strains and an HIV-1 mutant with a deletion of the V1/V2 region remains susceptible to 18A inhibition. A conformation-dependent gp120 target near the β20-β21 strands, which are highly conserved across HIV-1 isolates (Supplementary Fig. 12), is consistent with the available data. According to this model, interaction of 18A with this site restrains the CD4-induced movement of the V1/V2 region

that is required for transition of the HIV-1 Env trimer to the “open” conformation. The broad-range activity of 18A suggests that blockage of V1/V2 movement is not sensitive to sequence variation in the V1/V2 region of different HIV isolates.

The study of Env mutants with lower susceptibility to 18A inhibition revealed potential pathways to remove the block imposed by 18A on CD4-induced V1/V2 movement and gp41 HR1 exposure. Some reduced-susceptibility mutants demonstrated enhanced CD4-triggered movement of the V1/V2 region with low 18A-mediated restoration of the PG9 epitope, relative to that of the wild-type Env. One mutant, M434A, combined high resistance to the 18A-mediated blockade of both V1/V2 movement and gp41 HR1 exposure. Interestingly, low susceptibility to 18A was usually accompanied by increased envelope reactivity. As Env reactivity is inversely related to the activation barriers that maintain the unliganded state of Env, the alterations that reduce the responsiveness to 18A likely involve changes in Env conformation. However, increased Env reactivity is not sufficient for decreased sensitivity to 18A (Supplementary Fig. 9), suggesting that 18A interacts with regions that are specifically sensitive to alterations in the conformation of the unliganded Env trimer. Indeed, the phenotypes of the mutant Env panel suggest that multiple gp120 conformational states are able to be accommodated within functional Env trimers (Fig. 6).

In summary, 18A represents a valuable new probe to investigate different conformational states of HIV-1 Env and to define their importance to HIV-1 entry into cells. In our study, 18A inhibition demonstrated a wide coverage of diverse HIV-1 strains, and low susceptibility to 18A inhibition was accompanied by high envelope reactivity. Env mutants displaying reduced susceptibility to 18A inhibition exhibit enhanced sensitivity to neutralization by antibodies that do not neutralize wild-type HIV-1. The inverse relationship between 18A sensitivity and antibody sensitivity represents a potentially beneficial property. These types of antibodies are commonly elicited during natural HIV-1 infection and may synergize with 18A to limit pathways of HIV-1 escape. The attractive attributes of 18A make it a good candidate for further investigation, which should focus on efforts to improve the potency of 18A without compromising its breadth. An improved derivative with a higher therapeutic index (CC_{50}/IC_{50}) will allow further investigation of 18A resistance, which, for a few Envs, is partially masked by cytotoxicity at high concentrations. Initial studies show that the hydroxyl group is not absolutely required for antiviral activity, although it contributes to potency (Supplementary Table 5). Multiple diverse compounds containing the acylhydrazone moiety were inert in the screening assays, suggesting that this moiety can be well tolerated (Supplementary Fig. 13). Importantly, additional acylhydrazone-containing active compounds exhibited a different profile of resistance (Supplementary Figs. 14 and 15) and these may help to design improved derivatives of 18A in the future.

ONLINE METHODS

High-throughput screening (HTS)

We used the cell-cell fusion and specificity control assays in parallel to identify potential inhibitors of HIV-1 entry. Both assays were used to screen several libraries of chemical compounds from different sources (Supplementary Table S1) at the Institute of Chemistry and Cell Biology, Harvard Medical School.

HTS reagents—The following reagents were purchased from Invitrogen (Carlsbad, CA): Dulbecco's Modified Eagle Medium (DMEM) high glucose (cat# 11965–085), Roswell Park Memorial Institute (RPMI) 1640 (cat# 11875–085), DMEM high glucose without phenol red (cat# 31053–028), RPMI 1640 without phenol red (cat# 11835–030), Glutamax 200 mM (x100) (Cat# 35050), G418 (Geneticin® Selective Antibiotic, cat# 11811–031), and StemPro Accutase Cell Dissociation Reagent (cat# A11105–01). Tet System Approved FBS, US-Sourced (cat# 631101) and Doxycyline (cat# 631311) were purchased from Clontech (Mountain View, CA). Puromycin dihydrochloride from Streptomyces alboniger (cat# P8833–25MG) was purchased from Sigma-Aldrich (St. Louis, MO) and Steady-Glo substrate (cat# E2550) was purchased from Promega (Madison, WI).

HTS cell lines—H-JRFL#13[38] (effector) and H-Fluc4 (control) cells were grown in DMEM containing 10% FBS, 100 μg/ml streptomycin, 100 units/ml penicillin, 200 μg/ml G418, 1 μg/ml puromycin and 2 μg/ml doxycycline. H-JRFL#13 cells carry an HIV-1_{JR-FL} *env* gene that is induced by growing the cells in the absence of doxycycline (Tet-Off expression system). H-Fluc4 cells, which carry a *firefly luciferase* gene that is induced in the absence of doxycycline, were used as specificity controls. Both cell lines were derived from HeLa cells and constitutively express the tetracycline-regulated transactivator (Tet-Off expression system). CEM#21 target cells[38] were grown in RPMI containing 10% FBS, 100 μg/ml streptomycin, 100 units/ml penicillin and 1 μg/ml puromycin.

Primary screen—H-JRFL#13 or H-FLuc4 cells were washed thrice, detached with StemPro Accutase, centrifuged at 200 x g for 6 minutes at 10°C and seeded in DMEM containing 10% tetracycline-approved FBS, 100 μg/ml streptomycin, 100 units/ml penicillin, 100 μg/ml G418, 1 μg/ml puromycin and without Phenol Red. Medium was replaced after 3–6 hours to remove traces of doxycycline and cells were induced for a further 16–18 hours (40 hours for HFluc4 cells). Cells were washed and detached as above and 30 μl of 1.7×10^5 cells/ml in $RPMI_{assay}$ medium (RPMI containing 10% tetracycline-approved FBS, 100 μg/ml streptomycin, 100 units/ml penicillin, and without Phenol Red) were dispensed into 384-well plates. After an incubation of 2–4 hours, 100 nanoliters of the chemical compounds to be screened (the concentration of the compounds in each library is shown in Supplementary Table S1) were pin-transferred to the assay plate using a Seiko robot; doxcycline (4 μg/ml) and Maraviroc (a CCR5 inhibitor) (300 nM) were added manually to control wells. CEM#21 cells were centrifuged at 150 x g for 6 min and 15 μl of 8×10^5 cells/ml in $RPMI_{assay}$ medium were dispensed into each well of the 384-well plate. Following an incubation of 20 hours at 37°C, the plate was equilibrated to room temperature, 15 μl of Steady-Glo substrate (Promega) pre-diluted 1:1.5 in double-distilled water was added to each well, and the plate was incubated for an additional ~30 minutes at room temperature. Firefly luciferase activity was measured using an EnVision Multilabel Plate Reader (PerkinElmer, Boston, MA). Cells and substrates were dispensed into the 384-well plates using a Matrix WellMate (ThermoFisher Scientific, Waltham, MA) and all assays were performed in duplicate.

Secondary screen—A confirmatory screen of selected hits was performed similarly to the primary screen, but with the following modifications: 1) test compounds were

transferred using pocket tips (ThermoFisher Scientific), and 2) three assays were used in parallel: the cell-cell fusion assay, the specificity control assay, and a viability assay to measure potential cytotoxic effects of each compound on the CEM#21 cells (see viability assay below).

Analysis of screening data

For each compound, residual cell-cell fusion and residual specificity control activities measured in the primary and secondary screens were normalized using the equation:

$$\%\,\text{activity} = (\text{readout}_{\text{compound}} - \text{background}) / (\text{readout}_{\text{blank}} - \text{background}) \times 100$$

In this equation, % activity represents the residual activity in the cell-cell fusion assay or specificity control assay after incubation with the compound; $\text{readout}_{\text{compound}}$= measurement in the presence of the compound and $\text{readout}_{\text{blank}}$= measurement in the absence of the compound; background = measurement in the presence of doxycycline.

Readouts of duplicate measurements were used to calculate the mean and range of the % activity of each compound. Single concentration selectivity (SCS) was defined as the ratio of %Specificity:%Fusion and calculated for each compound. Compounds that resulted in: 1) %Fusion readout< (%Fusion without compound - 4 standard deviations) or 72.5%; and 2) SCS > $4.299 - (\%\text{Fusion} \times 0.0766) + (\%\text{Fusion}^2 \times 0.0004781)$ were selected for the secondary screen (this equation was empirically derived to exclude highly toxic compounds and retain selective compounds, even if their inhibition activity was weak; this function is plotted in broken red symbols in Fig. 1c,d). All data were processed and analyzed by a computer program written for this purpose in R.

Inhibition data were fitted to the four-parameter logistic equation using the nonlinear curve fit module in Origin 8.1 software (OriginLab, Northampton, MA), as previously described [39].

Chemical compounds

All compounds used in this study were purchased from commercial vendors and were >90% pure. Compounds 18A, 18A-4 (**5**), 18A-5 (**6**), 18A-6 (**7**) and 34A (**10**) were from Asinex, Moscow, Russia; compounds 18A-1 (**2**), 18A-2 (**3**), 18A-3 (**4**), 614 (**25**), 615 (**26**) and 617 (**28**) were from Enamine, Kiev, Ukraine; compounds 20CB (**8**), 27CB (**9**), 600 (**11**), 601 (**12**), 602 (**13**), 603 (**14**), 604 (**15**), 605 (**16**), 606 (**17**), 607 (**18**), 608 (**19**), 609 (**20**), 610 (**21**), 611 (**22**), 612 (**23**), 618 (**29**), 619 (**30**) and 622 (**33**) were from Chembridge, San Diego, CA; compounds 613 (**24**), 616 (**27**), 620 (**31**) and 621 (**32**) were from ChemDiv, San Diego, CA. All compounds were dissolved in sterile-filtered DMSO (Sigma, catalog number D2438) at 25 μM concentration and stored in aliquots at −80 °C.

Peripheral blood mononuclear cells (PBMC)

Human blood was purchased from Research Blood Components, who obtained a consent form from each donor, according to the American Association of Blood Banks guidelines. PBMC were isolated from the whole blood using a Ficoll-Paque gradient (Ficoll-Paque

PLUS, Amersham Biosciences) and activated at concentration of 10^6 live cells/ml for 3 days in RPMI-PBMC medium (RPMI-1640 supplemented with 20% FBS, 10% IL-2 (Hemagen, Columbia, MD), 100 μg/ml primocin (InvivoGen, San Diego, CA)) with 4 ug/ml phytohemagglutinin (Sigma-Aldrich, St. Louis, MO). In some cases, cells were frozen, thawed and activated prior to the assay.

Statistical analysis

A statistical parametric analysis was performed by unpaired Student's t-tests and ANOVA. A statistical non-parametric analysis was done by Spearman rank correlation and Mann–Whitney tests. A summary of the data statistics is included for each analysis in the relevant figure legend.

Construction of plasmids expressing JR-FL and KB9 Env chimeras

A plasmid for expression of the JR-FL gp120/KB9 gp41 Env chimera was built by digesting pCO-JRFLgp160 with XbaI and BsrGI restriction enzymes and subcloning the ~1500-bp (~1500-bp) JR-FL gp120-coding fragment into the same sites of pCO-KB9gp160. Similarly, an expression plasmid for the KB9 gp120/JR-FL gp41 env chimera was generated by digesting pCO-JRFLgp160 with BsrGI and AflII restriction enzymes and subcloning the ~1100-bp JR-FL gp41-coding fragment into pCO-KB9gp160, using the same sites. This strategy results in an Env chimera in which 22 amino acids upstream of the gp120-gp41 cleavage site is derived from the gp41-donating isolate. KB9(JR-FL V1-V5) and KB9(JR-FL C1-C5) chimeras contain the variable and constant regions of JR-FL gp120 engrafted into the KB9 Env, respectively. Each gene was constructed by PCR assembly of two block gene fragments (Integrated DNA technology, Coralville, Iowa) of the corresponding sequence. An overlapping short sequence allowed assembly of the DNA fragments and the PCR product was cut with XbaI and BsrGI restriction enzymes and cloned into the same sites of pCO-KB9gp160. The constructs expressing the chimeric Envs were confirmed by restriction site and DNA sequence analysis.

HIV-1 Env mutants

Mutations were introduced into the plasmid expressing the full-length HIV-1_{YU2} or HIV-1_{JR-FL} Envs using the QuikChange II site-directed mutagenesis protocol or the QuikChange multi site-directed mutagenesis kit (Stratagene). The presence of the desired mutations was confirmed by DNA sequencing. All HIV-1 Env residues are numbered based on alignment with the HXBc2 prototypic sequence, according to current convention.

To study CD4-independent infection, the full-length HIV-1_{ADA} N197S Env mutant was used. This Env is an ADA-HXBc2 chimera with an N197S change[18]. The control "wild-type" ADA Env used in these experiments is also an ADA-HXBc2 chimera[18].

Production of recombinant HIV-1 expressing luciferase

293T cells were cotransfected with an Env expression plasmid, a firefly luciferase-expressing lentiviral vector (pHIVec2.luc) and an HIV-1-based packaging plasmid (psPAX2, cat# 11348, NIH AIDS Research and Reference Reagent Program) at a ratio of 1:6:3 using Effectene (Qiagen, Germantown, MD). After 48 hours, the supernatant was

collected, buffered with 50 mM Hepes pH 7.4 (final concentration) and centrifuged for 5 minutes at 750 x g and 4°C. The virus-containing supernatant was used directly or frozen at −80°C.

Viral infection assay

Each test compound was serially diluted in DMSO in a 96-well B&W isoplate (PerkinElmer, Boston, MA) using an HP D300 Digital Dispenser, to a final volume of 450 nl. DMSO was used as a control. Viruses pseudotyped with a specific Env were added to each well and incubated briefly at room temperature. Cf2Th-CD4/CCR5 cells were detached with StemPro Accutase Cell Dissociation Reagent (Invitrogen, cat# A11105–01), washed once, and 5000 cells were added to each well. After 3–4 hour incubation at 37°C, the viruses and compounds were removed, the medium was replaced and the cells were further incubated for a total of 24–30 hours (in a few cases, cells were incubated for a total of 44 hours; when the experiment was repeated with an incubation period of 30 hours, no differences in 18A inhibition were observed). Following incubation, the medium was aspirated and cells were lysed with 30 µl of Passive Lysis Buffer (Promega, cat# E1941). The activity of the firefly luciferase, which was used as a reporter protein in the system, was measured with a Centro LB 960 luminometer (Berthold Technologies, Oak Ridge, TN). One hundred microliters of assay buffer (15 mM $MgSO_4$, 15 mM KH_2PO_4/K_2HPO_4 pH 7.8, 1 mM ATP and 1 mM DTT) was injected to each well, followed by a 50 µl injection of 1 mM D-luciferin potassium salt (BD Pharmingen, San Jose, CA); luminescence was measured for 2 sec. Infection of PBMC was done as above, but 20,000–40,000 cells/well and viruses concentrated by ultracentrifugation were used. After four hours of incubation with viruses, the cells were centrifuged at 200 x g for 6 minutes at 4°C, resuspended in 100 µl RPMI-PBMC medium and incubated at 37°C for an additional 36–40 hours (total 40–44 hours). Supernatant was removed after centrifugation at 400 x g for 5 minutes and cells were processed to detect luciferase activity, as described above.

For washout experiments, different concentrations of 18A were incubated with the recombinant viruses at 37°C for 20 minutes. The viruses were laid on a 20% sucrose cushion and ultracentrifuged at 30,000 RPM in an SW55 rotor for 1.5 hours at 4°C. After the supernatant was aspirated, viruses were suspended in 500–1000 µl medium and 90 µl of the virus suspension was used to infect 5000 Cf2Th-CD4/CCR5 cells (5 replicates). The cells were incubated for 48 hours and processed as described above.

Sensitivity of recombinant viruses to cold inactivation was measured as previously described[25].

Viability Assay

As part of the secondary screen, cells were incubated for ~20 hours in 384-well plates in a final volume of 45 µl growth medium at 37°C. The plate was equilibrated to room temperature, 15 µl of CellTiterGlo (Promega) was added to each well and luminescence was measured as described above. The viability assay with 18A was done in parallel to the viral infection assay for the same length of time. 18A was diluted using an HP D300 Digital Dispenser in a 96-well B&W isoplate and cells were added. After incubation of 26–30 hours

(Cf2Th cells) or 40–44 hours (PBMC), 30 μl (Cf2Th cells) or 100 μl (PBMC) of CellTiterGlo was added and luminescence was measured as described above.

HIV-1_{JR-FL} gp120 purification

A pcDNA3.1(−)Zeo based plasmid encoding the gp120 glycoprotein of HIV-1_{JR-FL} was transfected into 293F cells using 293fectin (Invitrogen), according to the manufacturer's instructions. The gp120 glycoprotein, which contains a 6-histidine tag at the C terminus, was purified from the culture supernatant after 6 days using Ni-NTA chromatography.

Western blotting

Purified HIV-1_{JR-FL} gp120 was separated on 8–16% Tris-glycine gel, transfer to a nitrocellulose membrane and detected with a 1:10,000 dilution of serum from an HIV-1-infected individual, followed by a 1:10,000 dilution of peroxidase-conjugated F(ab′)2 fragment donkey anti-human IgG (catalog no. 706–036–098; Jackson ImmunoResearch Laboratories).

Enzyme-linked immunosorbent assay (ELISA)

A white, high-binding microtiter plate (Corning) was coated by incubating 0.125 μg of mouse anti-polyhistidine antibody (Catalog no. sc-53073, Santa Cruz Biotechnology) diluted to a final concentration of 1.25 μg/ml in 100 μl PBS in each well overnight. Wells were blocked with blocking buffer (5% nonfat dry milk (Bio-Rad) in PBS) for 2 hours and then washed twice with PBS. Between 0.25 and 0.5 μg of purified HIV-1_{JR-FL} gp120 in blocking buffer was added to each well; the plate was incubated for 60 minutes and washed thrice with PBS. Eighty microliters of either DMSO or 18A (at concentrations of either 21.4 or 86 μM) in blocking buffer were added to the wells and after a 30-minute incubation, 20 μl of the specified antibody in blocking buffer was added. The plate was incubated for a further 30 minutes and washed thrice with 0.05% Tween in PBS and thrice with PBS. Peroxidase-conjugated $F(ab')_2$ fragment donkey anti-human IgG (1:3,600 dilution; catalog no. 706–036–098; Jackson ImmunoResearch Laboratories) in blocking buffer was added to each well. The plate was incubated for 30 minutes, washed three times with 0.05% Tween in PBS and three times with PBS, as before, and 80 μl of SuperSignal chemiluminescent substrate (Pierce) was added to each well. The relative light units in each well were measured for 2 sec with a Centro LB 960 luminometer (Berthold Technologies). All procedures were performed at room temperature. Cell-based ELISA was performed as previously described[25].

Circular dichroism (CD) analysis

CD spectra of the HIV-1_{JR-FL} gp120 glycoprotein were measured in the presence of 25 μM test compound or DMSO at 20°C with a quartz cell with a 1-mm path length (Starna Cells Inc, Atascadero, CA) using a JASCO J-815 CD Spectrometer (JASCO Inc, Easton, MD). The HIV-1_{JR-FL} gp120 glycoprotein was diluted to 4.6 μM in 20 mM Tris-HCl, pH 8.0 and a test compound or DMSO was added to the solution. The final DMSO concentration in all samples was 0.1%. Each spectrum was measured in at least two independent experiments

and represents the average of at least 25 cycles of scanning between wavelengths of 200 nm and 250 nm.

Flow cytometry

Plasmids expressing the wild-type HIV-1_{JR-FL}ΔCT Env or the double mutant HIV-1_{JR-FL} E168K+N188AΔCT Env were transfected with the Effectene transfection reagent (Qiagen) into 293T cells, according to the manufacturer's instructions. After 48–72 hours, cells were detached with 5 mM EDTA/PBS and between 0.5–1 million cells were briefly incubated with various concentrations of 18A and then with or without the indicated concentrations of sCD4. C34-Ig (at a final concentration of 20 μg/ml) or a specified antibody (at final concentration of 1 μg/ml) was added to the cells. After a 30-minute incubation, the cells were washed twice and incubated with Allophycocyanin-conjugated $F(ab')_2$ fragment donkey anti-human IgG antibody (1:100 dilution; catalog no. 709–136–149; Jackson ImmunoResearch Laboratories) and Fluorescein isothiocyanate-conjugated anti-CD4 antibody (1:33 dilution, E-biosciences) for 15 minutes. Cells were washed twice and analyzed with a BD FACSCanto II flow cytometer (BD Biosciences). For analysis of Env mutants with reduced sensitivity to 18A (Fig. 5d–e), the measurements were normalized for the level of sCD4 binding of each mutant, and the response of each mutant was further normalized to that of the wild-type HIV-1_{JR-FL} E168K+N188AΔCT Env (herein designated WT_{KA}). In the absence of sCD4, the binding of C34-Ig to cells expressing the wild-type and mutant Envs was similar to that of the control cells without Env. The sCD4 IC_{50}/sCD4 binding ratio (Fig. 4b and Supplementary Fig. 7a) was calculated as follows. Binding of sCD4 to different envelope mutants was measured by flow cytometry and normalized first to 2G12 binding to account for potentially different Env expression levels, and then to sCD4 binding to the wild-type HIV-1_{JR-FL} Env. The IC_{50} of sCD4 for inhibition of virus infection by each mutant Env was divided by the normalized sCD4 binding to Env-expressing cells to calculate the sCD4 IC_{50}/sCD4 binding value.

Binding of soluble JR-FL gp120 to CCR5 was tested by incubating 1 million Cf2Th-CCR5 cells with 20 μg/ml purified gp120 in the presence or absence of 20 μg/mL sCD4 for 1 hour. After two washes, the cells were incubated with the 2G12 antibody followed by Allophycocyanin-conjugated $F(ab')_2$ fragment donkey anti-human IgG antibody to detect bound gp120. The cells were analyzed by FACS. All procedures were performed at room temperature.

Supplementary Material

Refer to Web version on PubMed Central for supplementary material.

Acknowledgments

We thank Y. McLaughlin and E. Carpelan for manuscript preparation; the AIDS Research and Reference Reagent Program, Division of AIDS, NIAID, NIH for providing reference panels for subtype B and C HIV-1 envelope clones, CFR01_AE.269 HIV-1 envelope clone, psPAX2 plasmid, T20, Maraviroc, and CEM cells. We also thank B. Keele, G.M. Shaw and the Center for HIV-AIDS Vaccine Immunology Consortium for providing transmitted/founder HIV-1 envelope clones; H-X. Liao and B.F. Haynes from Duke University Medical Center, Durham, NC for providing the CRF01_AE.CM244 HIV-1 envelope clone; D. Flood, J. Smith and C. Shamu from the Institute of Chemistry and Cell Biology at Harvard Medical School for assistance in the high-throughput screening campaign;

and E. Pery, E. Cassol, V. Misra, N. Madani, H. Haim, and A.M Princiotto from Dana-Farber Cancer Institute for helpful discussions and for providing reagents. A.H. was supported by amfAR and is the recipient of an amfAR Mathilde Krim Fellowship in Basic Biomedical Research (108501-53-RKNT). A.F. was supported by CIHR operating grant number 257792 and is the recipient of a FRSQ Chercheur Boursier Junior fellowship number 24639. Support for this work was also provided by grants from the National Institutes of Health to J.G.S (grant numbers AI24755 and GM56550).

References

1. Barre-Sinoussi F, et al. Isolation of a T-lymphotropic retrovirus from a patient at risk for acquired immune deficiency syndrome (AIDS). Science. 1983; 220:868–71. [PubMed: 6189183]
2. Gallo RC, et al. Frequent detection and isolation of cytopathic retroviruses (HTLV-III) from patients with AIDS and at risk for AIDS. Science. 1984; 224:500–3. [PubMed: 6200936]
3. Choe H, et al. The beta-chemokine receptors CCR3 and CCR5 facilitate infection by primary HIV-1 isolates. Cell. 1996; 85:1135–48. [PubMed: 8674119]
4. Dalgleish AG, et al. The CD4 (T4) antigen is an essential component of the receptor for the AIDS retrovirus. Nature. 1984; 312:763–7. [PubMed: 6096719]
5. Dragic T, et al. HIV-1 entry into CD4+ cells is mediated by the chemokine receptor CC-CKR-5. Nature. 1996; 381:667–73. [PubMed: 8649512]
6. Feng Y, Broder CC, Kennedy PE, Berger EA. HIV-1 entry cofactor: functional cDNA cloning of a seven-transmembrane, G protein-coupled receptor. Science. 1996; 272:872–7. [PubMed: 8629022]
7. Furuta RA, Wild CT, Weng Y, Weiss CD. Capture of an early fusion-active conformation of HIV-1 gp41. Nat Struct Biol. 1998; 5:276–9. [PubMed: 9546217]
8. He Y, et al. Peptides trap the human immunodeficiency virus type 1 envelope glycoprotein fusion intermediate at two sites. J Virol. 2003; 77:1666–71. [PubMed: 12525600]
9. Koshiba T, Chan DC. The prefusogenic intermediate of HIV-1 gp41 contains exposed C-peptide regions. J Biol Chem. 2003; 278:7573–9. [PubMed: 12486032]
10. Kwon YD, et al. Unliganded HIV-1 gp120 core structures assume the CD4-bound conformation with regulation by quaternary interactions and variable loops. Proc Natl Acad Sci U S A. 2012; 109:5663–8. [PubMed: 22451932]
11. Madani N, et al. Small-molecule CD4 mimics interact with a highly conserved pocket on HIV-1 gp120. Structure. 2008; 16:1689–701. [PubMed: 19000821]
12. Lin PF, et al. A small molecule HIV-1 inhibitor that targets the HIV-1 envelope and inhibits CD4 receptor binding. Proc Natl Acad Sci U S A. 2003; 100:11013–8. [PubMed: 12930892]
13. Si Z, et al. Small-molecule inhibitors of HIV-1 entry block receptor-induced conformational changes in the viral envelope glycoproteins. Proc Natl Acad Sci U S A. 2004; 101:5036–41. [PubMed: 15051887]
14. LaLonde JM, et al. Structure-based design, synthesis, and characterization of dual hotspot small-molecule HIV-1 entry inhibitors. J Med Chem. 2012; 55:4382–96. [PubMed: 22497421]
15. Regueiro-Ren A, et al. Inhibitors of human immunodeficiency virus type 1 (HIV-1) attachment. 12. Structure-activity relationships associated with 4-fluoro-6-azaindole derivatives leading to the identification of 1-(4-benzoylpiperazin-1-yl)-2-(4-fluoro-7-[1,2,3]triazol-1-yl-1h-pyrrolo[2,3-c]pyridin-3-yl)ethane-1,2-dione (BMS-585248). J Med Chem. 2013; 56:1656–69. [PubMed: 23360431]
16. Schader SM, et al. HIV gp120 H375 is unique to HIV-1 subtype CRF01_AE and confers strong resistance to the entry inhibitor BMS-599793, a candidate microbicide drug. Antimicrob Agents Chemother. 2012; 56:4257–67. [PubMed: 22615295]
17. Keele BF, et al. Identification and characterization of transmitted and early founder virus envelopes in primary HIV-1 infection. Proc Natl Acad Sci U S A. 2008; 105:7552–7. [PubMed: 18490657]
18. Kolchinsky P, Kiprilov E, Bartley P, Rubinstein R, Sodroski J. Loss of a single N-linked glycan allows CD4-independent human immunodeficiency virus type 1 infection by altering the position of the gp120 V1/V2 variable loops. J Virol. 2001; 75:3435–43. [PubMed: 11238869]

19. Julien JP, et al. Broadly neutralizing antibody PGT121 allosterically modulates CD4 binding via recognition of the HIV-1 gp120 V3 base and multiple surrounding glycans. PLoS Pathog. 2013; 9:e1003342. [PubMed: 23658524]
20. Wyatt R, et al. The antigenic structure of the HIV gp120 envelope glycoprotein. Nature. 1998; 393:705–11. [PubMed: 9641684]
21. Xiang SH, et al. Epitope mapping and characterization of a novel CD4-induced human monoclonal antibody capable of neutralizing primary HIV-1 strains. Virology. 2003; 315:124–34. [PubMed: 14592765]
22. Zhou T, et al. Structural basis for broad and potent neutralization of HIV-1 by antibody VRC01. Science. 2010; 329:811–7. [PubMed: 20616231]
23. Rizzuto CD, et al. A conserved HIV gp120 glycoprotein structure involved in chemokine receptor binding. Science. 1998; 280:1949–53. [PubMed: 9632396]
24. Julien JP, et al. Crystal Structure of a Soluble Cleaved HIV-1 Envelope Trimer. Science. 2013
25. Haim H, et al. Contribution of intrinsic reactivity of the HIV-1 envelope glycoproteins to CD4-independent infection and global inhibitor sensitivity. PLoS Pathog. 2011; 7:e1002101. [PubMed: 21731494]
26. McGee K, et al. The selection of low envelope glycoprotein reactivity to soluble CD4 and cold during simian-human immunodeficiency virus infection of rhesus macaques. J Virol. 2014; 88:21–40. [PubMed: 24131720]
27. Scott CF Jr, et al. Human monoclonal antibody that recognizes the V3 region of human immunodeficiency virus gp120 and neutralizes the human T-lymphotropic virus type IIIMN strain. Proc Natl Acad Sci U S A. 1990; 87:8597–601. [PubMed: 1700435]
28. Haim H, et al. Modeling virus- and antibody-specific factors to predict human immunodeficiency virus neutralization efficiency. Cell Host Microbe. 2013; 14:547–58. [PubMed: 24237700]
29. Kassa A, et al. Identification of a human immunodeficiency virus type 1 envelope glycoprotein variant resistant to cold inactivation. J Virol. 2009; 83:4476–88. [PubMed: 19211747]
30. Kassa A, et al. Transitions to and from the CD4-bound conformation are modulated by a single-residue change in the human immunodeficiency virus type 1 gp120 inner domain. J Virol. 2009; 83:8364–78. [PubMed: 19535453]
31. Doores KJ, Burton DR. Variable loop glycan dependency of the broad and potent HIV-1-neutralizing antibodies PG9 and PG16. J Virol. 2010; 84:10510–21. [PubMed: 20686044]
32. Walker LM, et al. Broad and potent neutralizing antibodies from an African donor reveal a new HIV-1 vaccine target. Science. 2009; 326:285–9. [PubMed: 19729618]
33. McLellan JS, et al. Structure of HIV-1 gp120 V1/V2 domain with broadly neutralizing antibody PG9. Nature. 2011; 480:336–43. [PubMed: 22113616]
34. Julien JP, et al. Asymmetric recognition of the HIV-1 trimer by broadly neutralizing antibody PG9. Proc Natl Acad Sci U S A. 2013; 110:4351–6. [PubMed: 23426631]
35. Walker LM, et al. Broad neutralization coverage of HIV by multiple highly potent antibodies. Nature. 2011; 477:466–70. [PubMed: 21849977]
36. Liu J, Bartesaghi A, Borgnia MJ, Sapiro G, Subramaniam S. Molecular architecture of native HIV-1 gp120 trimers. Nature. 2008; 455:109–13. [PubMed: 18668044]
37. Pettersen EF, et al. UCSF Chimera--a visualization system for exploratory research and analysis. J Comput Chem. 2004; 25:1605–12. [PubMed: 15264254]
38. Herschhorn A, et al. An inducible cell-cell fusion system with integrated ability to measure the efficiency and specificity of HIV-1 entry inhibitors. PLoS One. 2011; 6:e26731. [PubMed: 22069466]
39. Herschhorn A, Hizi A. Virtual screening, identification, and biochemical characterization of novel inhibitors of the reverse transcriptase of human immunodeficiency virus type-1. J Med Chem. 2008; 51:5702–13. [PubMed: 18800765]

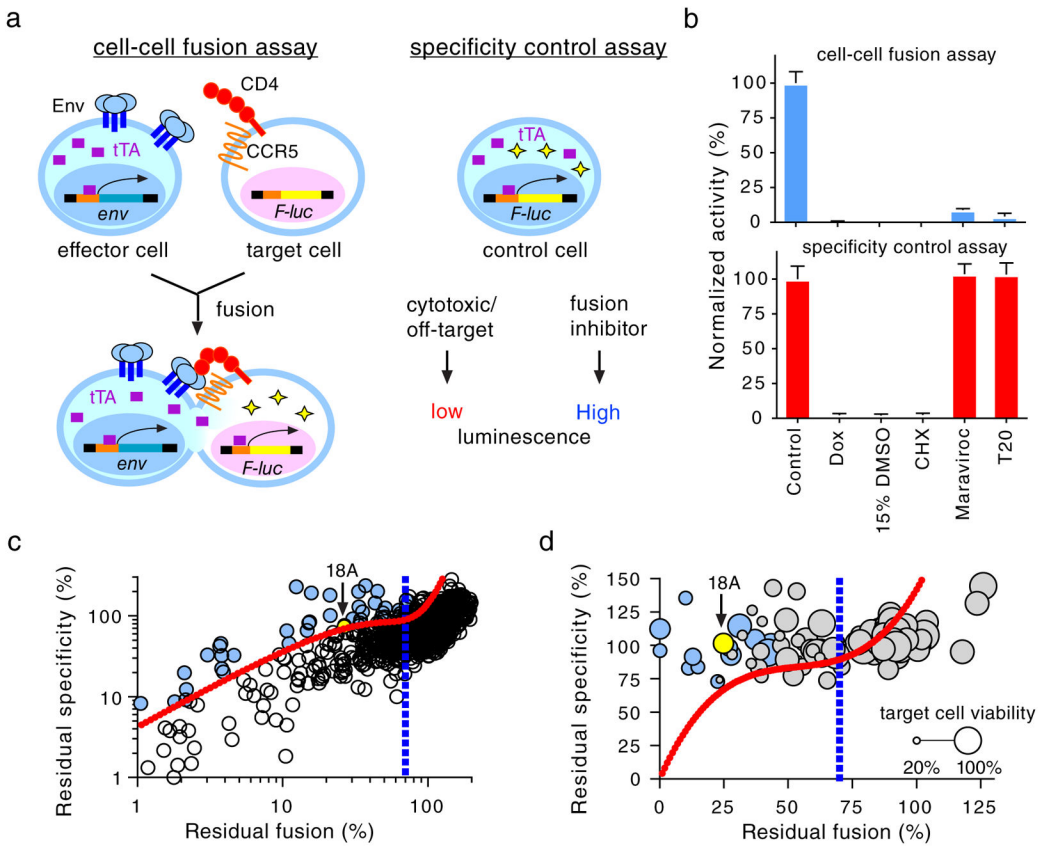

Figure 1. Screening assay and data analysis

(**a**) Cell-cell fusion and specificity control assays. In the cell-cell fusion assay (left, adapted from reference 38), Env-mediated membrane fusion enables diffusion of a tetracycline-regulated transactivator (tTA) that activates firefly luciferase (F-luc) expression in the target cells. In the specificity control assay (right) used as a counterscreen, F-luc is induced to allow measurement of any off-target effects. (**b**) The two assays were validated with known HIV-1 entry inhibitors (Maraviroc and T20) and cytotoxic/off-target compounds. Dox, doxycycline (a tTA inhibitor), CHX, cycloheximide. (**c**) Data from primary screen. The readout of each test compound was normalized to the assay readout without a compound. The effect of each compound on the cell-cell fusion assay versus its effect on the specificity control assay was plotted. A filter for inhibition (blue line) and a specificity threshold (red line, high ratio of normalized residual specificity to normalized residual inhibition) were applied to all compounds. Hits are identified in light blue at the top left portion of the plot. Analysis of ~8000 out of 212,285 screened compounds is shown. (**d**) Data from secondary screen. Identified hits were retested in the cell-cell fusion and specificity assays and, in addition, were tested for any effect on target cell viability. The results are plotted as in **c,** but the size of each circle indicates the effect of each compound on target cell viability. Confirmed inhibitors that showed high selectivity and were not cytotoxic to the target cells are shown in light blue. 18A is shown in yellow.

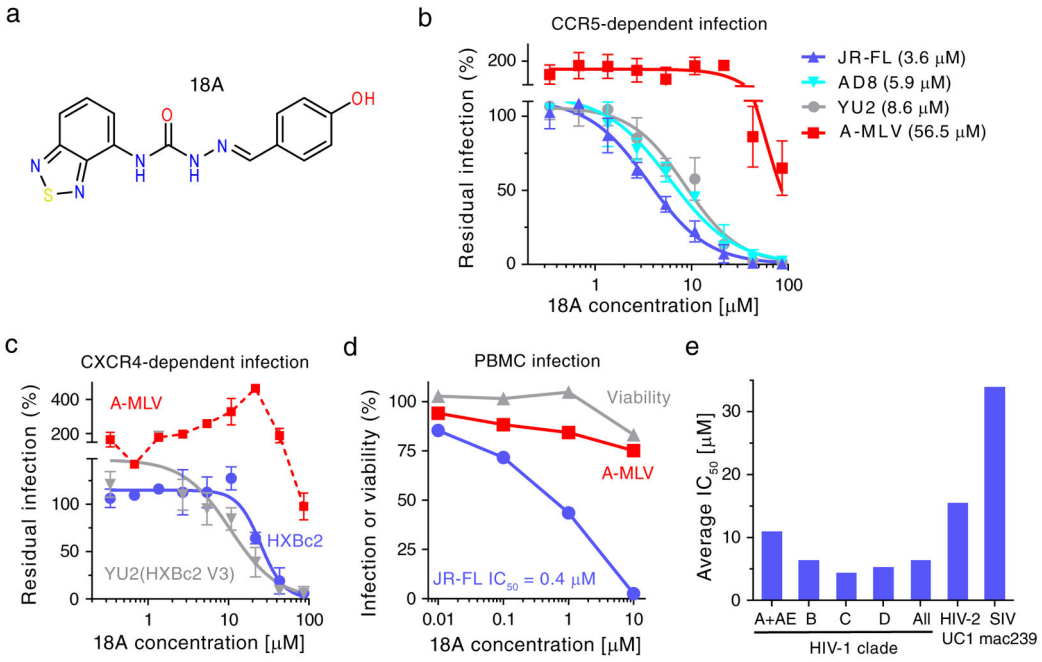

Figure 2. Effects of 18A on infection of R5- and X4-tropic viruses

(**a**) Structure of 18A. (**b**) The effect of 18A on infection of Cf2Th-CD4/CCR5 cells by R5 HIV-1. (**c**) Same as (**b**), but using CXCR4-tropic viruses and Cf2Th-CD4/CXCR4 cells. Infection of the control A-MLV was enhanced at low concentrations and steeply decreased at higher concentrations; we could not fit the data to a standard inhibition curve, but in a separate experiment, the measured CC_{50} of 18A for these cells was 63 μM. (**d**) Specific inhibition of HIV-1_{JR-FL} infection of human PBMC by 18A. (**e**) Average IC_{50} values of 18A inhibition for CCR5-using HIV-1 from the indicated phylogenetic clades, for all CCR5-using HIV-1 isolates, and for other primate immunodeficiency viruses (see Supplementary Table 3 for the IC_{50} of each isolate).

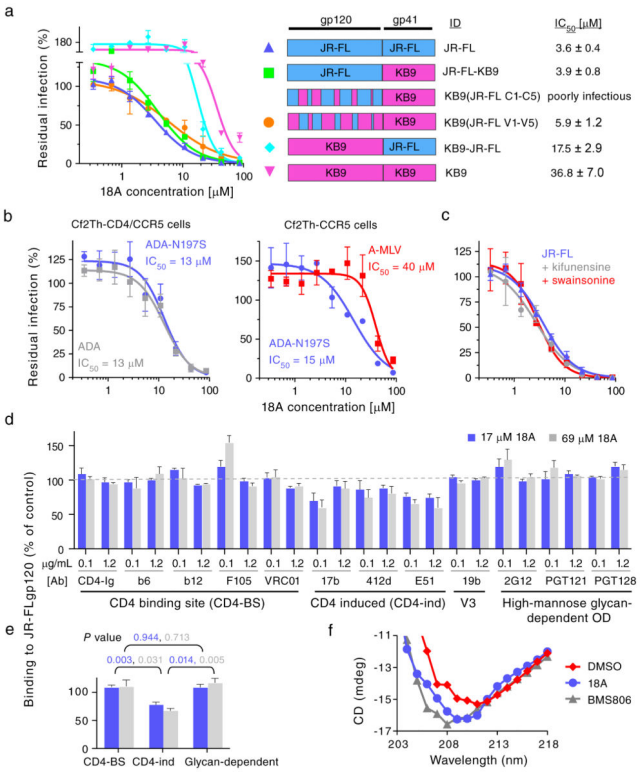

Figure 3. Investigation of the target of 18A inhibition

(**a**) Chimeras between HIV-1 strains displaying high (JR-FL) and low (KB9) sensitivity to 18A were tested for inhibition by 18A. (**b**) The requirement of 18A inhibition for CD4 was tested by challenging CD4/CCR5-expressing cells and CCR5-expressing cells with the CD4-independent HIV-1_{ADA} N197S mutant. (**c**) The dependence of 18A inhibition on complex glycans on HIV-1 Env was measured by preparing recombinant JR-FL viruses in the presence and absence of two glycosidase inhibitors and testing their sensitivity to 18A. (**d**) Profile of binding of a large panel of monoclonal antibodies with known epitopes to the 18A-bound gp120 glycoprotein. Binding was normalized to the antibody binding in the absence of 18A. OD, outer domain. (**e**) Analysis of the interference of 18A with antibody binding. The monoclonal antibodies from (**d**) were grouped according to their binding site on gp120 and the effect of 18A on their binding at a concentration of 0.1 μg/ml was averaged. An ANOVA test for significant differences between the means of the groups showed *P* values of 0.003 and 0.015 for the 17 μM and 69 μM concentrations of 18A, respectively. The *P* values shown were calculated using Student's t test; light blue and gray correspond to the 17 μM and 69 μM concentrations of 18A, respectively. (**f**) Circular dichroism analysis of HIV-1_{JR-FL} gp120 in the presence of DMSO (a negative control), 18A or BMS-806 (a positive control). The data shown are means ± SEM (**a–e**) or representative (**f**) of 2–5 independent experiments.

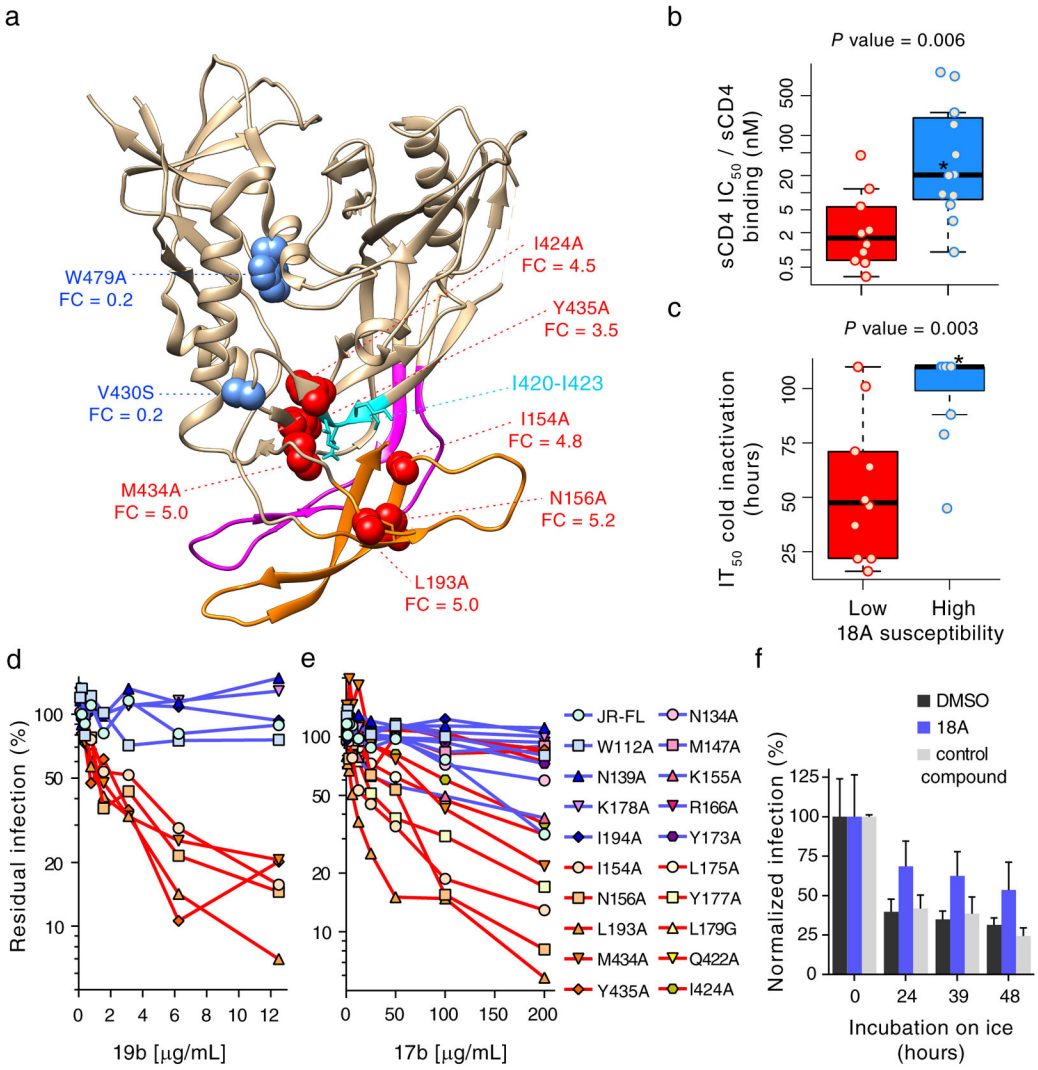

Figure 4. Effect of gp120 changes on HIV-1 sensitivity to 18A

(**a**) Amino acid residues associated with low (red) or high (light blue) sensitivity to 18A are shown on the crystal structure of the BG505 SOSIP.664 soluble gp140 (PDB 4NC0). FC (fold change) is the ratio of mutant to wild-type IC_{50} values; IC_{50} value of each isolate is shown in Supplementary Table 4. The IKQI sequence, which is shared by the epitopes of the CD4i antibodies, is shown in cyan. V3 region, magenta; V1/V2 region, orange. The Env structure was displayed using the UCSF Chimera package[37]. (**b,c**) Soluble CD4 (sCD4) inhibition (**b**) and cold inactivation (**c**) of virus mutants with low (red) and high (light blue) sensitivity to 18A (see Supplementary Fig. 8). The Mann-Whitney test was used to calculate the indicated *P* values; black bar, median; the boxes include the first, second and third quartiles; whiskers are extended to the interquartile range from the box; IT_{50}, half-life on ice. Asterisks (**b–c**), wild-type HIV-1_{JR-FL} Env. (**d,e**) Neutralization by the 19b (**d**) and 17b (**e**) antibodies of HIV-1 Env mutants with low (red) and high (light blue) sensitivity to 18A. (**f**) Infectivity of a recombinant virus with the HIV-1_{HXBc2} Env after preincubation on ice for the indicated times.

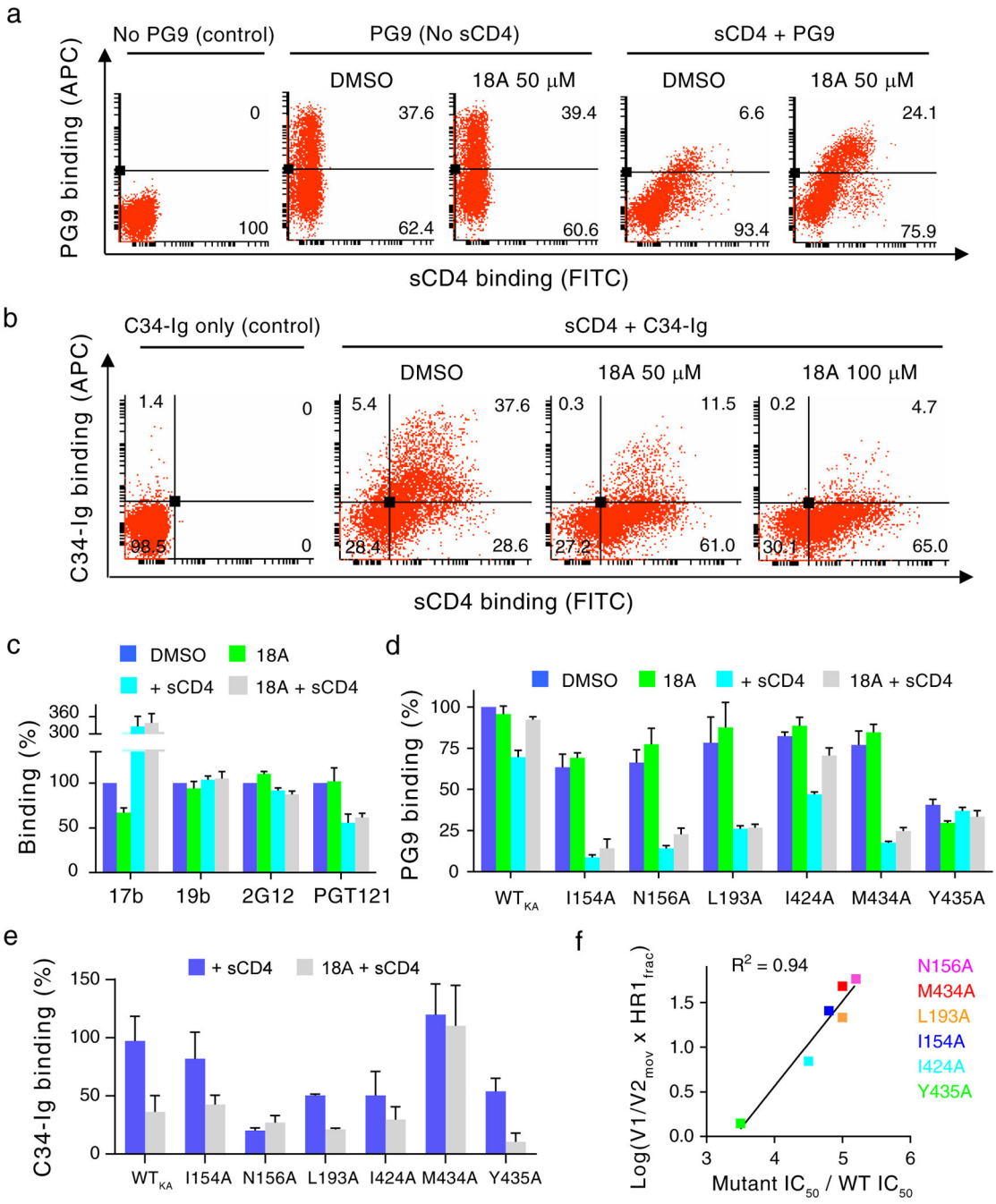

Figure 5. Mechanism of 18A inhibition of HIV-1 infection

(**a**) The effect of 18A on the binding of the PG9 antibody to the cell-surface HIV-1_{JR-FL} E168K+N188AΔCT Env trimer (designated WT_{KA}) in the presence or absence of sCD4, measured by two-color flow cytometry. Control, secondary antibody only. APC, allophycocyanin; FITC, fluorescein isothiocyanate. (**b**) The effect of 18A on CD4-induced gp41 HR1 exposure in the cell-surface HIV-1_{JR-FL}ΔCT Env trimer. Additional controls for the mode of inhibition are shown in Supplementary Figure 9. (**c**) The effect of 18A on binding of the indicated antibodies to HIV-1_{JR-FL} WT_{KA} Env. Normalized mean

fluorescence intensity is shown. (**d–f**) Mechanism of resistance to 18A using HIV-1_{JR-FL} WT_{KA} and HIV-1_{JR-FL} WT_{KA} mutants with reduced sensitivity to 18A. (**d**) The effect of 18A on PG9 binding was examined as in (**c**). (**e**) The effect of 18A on the sCD4-induced gp41 HR1 exposure. (**f**) Correlation between fold decrease in susceptibility to 18A inhibition and the integrated ability of 18A to counteract CD4-induced V1/V2 rearrangement ($V1/V2_{mov}$= decrease – restoration of PG9 binding) and HR1 exposure ($HR1_{frac}$= HR1 exposure in the presence / HR1 exposure in the absence of 18A). Data shown are representative (**a, b**) or average (all other panels) results from 2–4 independent experiments.

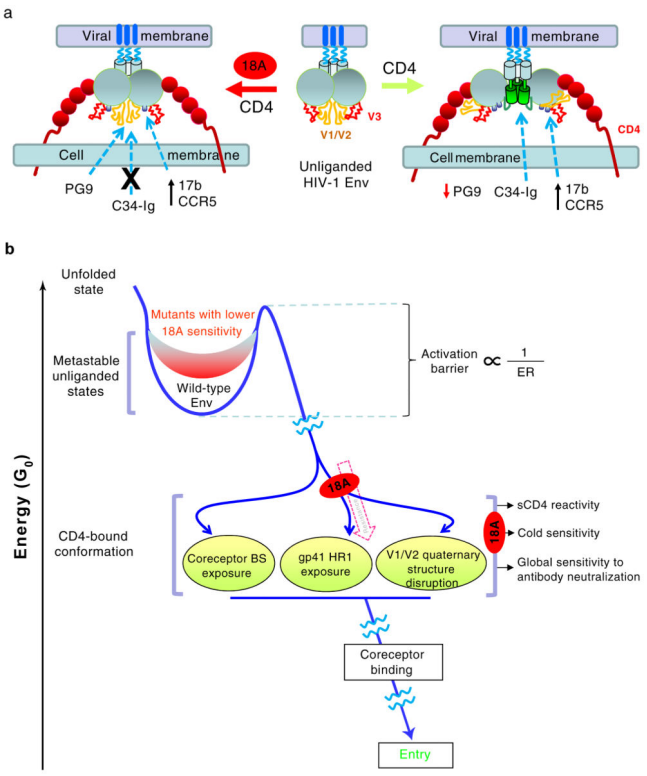

Figure 6. Model for the inhibition of HIV-1 entry by 18A

(**a**) Molecular mechanism of 18A inhibition. Binding to CD4 “opens” the HIV-1 Env trimer and induces V1/V2 movement and gp41 HR1 exposure, which can be detected by a decrease in the binding of the PG9 antibody and an increase in the binding of C34-Ig, respectively (right). Interaction of 18A with the HIV-1 Env prior to CD4 engagement blocks the V1/V2 movement and gp41 HR1 exposure (left). (**b**) Interaction points of 18A with HIV-1 Env along the entry pathway. The postulated free energies associated with the metastable unliganded states of the wild-type Env and Env variants with decreased 18A sensitivity are indicated. Compared with the wild-type Env, the Env mutants with decreased 18A sensitivity exhibit higher envelope reactivity and a lower activation barrier separating the unliganded states from downstream conformations. The proposed points of 18A inhibition of Env movement into the CD4-bound conformation are indicated. BS, binding site.